

# A Preprocessing Filter to Improve Super Paramagnetic Iron Oxide Nanoparticle (SPION): Based Early Tumor Detection

Mehdi Baqri<sup>1\*</sup>, Sri Kamal K andala<sup>2</sup> and David Fuentes<sup>2</sup>

<sup>1</sup>Department of Biomedical Engineering, Yale University, New Haven, USA

<sup>2</sup>Department of Imaging Physics, University of Texas MD Anderson Cancer Center, Houston, USA

## Abstract

The early detection of aggressive forms of ovarian cancer before they metastasize is critical for reducing overall mortality from the disease. Super Paramagnetic Relaxometry (SPMR) is an imaging technique useful for visualizing early stage tumors with high sensitivity and specificity. It uses Superconducting Quantum Interference Devices (SQUIDs) to detect targeted Superparamagnetic Iron Oxide Nanoparticles (SPIONs) that visualize tumors ten times smaller than what conventional imaging techniques can. However, the ultra-sensitivity of SQUIDs increases their risk of distortion due to far-field artifacts. Therefore, a preprocessing filter was developed to mitigate far-field, low-frequency disturbances to SQUID signal acquisition. This is based on the hypothesis that correcting SQUID signal acquisition using a magnetometer for far-field detection will increase the accuracy of SPMR for early tumor detection. The hypothesis was tested in three steps. First, it was shown that the Magnetometer (MAG) could specifically detect far-field noise and effectively avoid Nanoparticle (NP) signatures. Second, low-frequency noise was induced to show that far-field artifacts in the MAG signal correlated with distortions in the SQUID channels. Therefore, a preprocessing filter was developed to parse through and parameterize MAG signal extrema to SQUID signal distortions. A series of further optimization steps included anchoring the MAG signal to respective channels, modelling and subtracting the component of structural (environmental) relaxation and constraining a general subtraction window. Third, success was measured by the image reconstruction accuracy of sources with various NP concentrations, using the HSPMR dipole-fitting technique. Overall, the MAG-filter increased reconstruction accuracy more effectively with decreasing NP signal; accuracy increased the most at very low concentrations (~1 $\mu$ g). This preliminary data indicate that the filter increases SPMR sensitivity for low NP concentrations representative of small cell clusters, typical of early disease stages. Future work will optimize this initial filter to work uniformly and effectively across different NP concentrations (and tumor sizes) and translate this technology to highly sensitive early tumor detection.

**Keywords:** Modelling • Magnetometer • Nanoparticle • Superparamagnetic

## Introduction

The early detection of aggressive forms of ovarian cancer is critical for reducing overall mortality from the disease. A major factor of this is the propensity of Type II carcinomas to metastasize from microscopic lesions. Early detection of these and other carcinomas requires highly sensitive technology that current screening methods lack. Superparamagnetic Relaxometry (SPMR) is a promising tool for highly sensitive detection of tumor cells that may improve early stage detection of cancers. It uses the magnetic properties of Superparamagnetic Iron Oxide Nanoparticles (SPIONs)

and relaxation-based discrimination to locate and differentiate cancer cells [1].

SPMR achieves specificity by using antibodies or mechanisms of cell uptake to target Nanoparticles (NPs) to cancer cells. Magnetic NPs are useful because they are stable, nontoxic and can be used on opaque media. SPMR leverages highly sensitive Superconducting Quantum Interference Devices (SQUIDs) to localize NPs bound to as few as 15,000 cancer cells, ten times smaller than what conventional methods can detect. Significant studies have augmented this technology by calibrating SQUID

**\*Address for Correspondence:** Mehdi Baqri, Department of Biomedical Engineering, Yale University, New Haven, USA; E-mail: mehdi.baqri@yale.edu

**Copyright:** © 2022 Baqri M, et al. This is an open-access article distributed under the terms of the creative commons attribution license which permits unrestricted use, distribution and reproduction in any medium, provided the original author and source are credited.

**Received:** April 24, 2020, Manuscript No. jme-20-9736; **Editor assigned:** April 27, 2020, PreQC No. jme-20-9736 (PQ); **Reviewed:** May 11, 2020, QC No. jme-20-9736; **Revised:** August 25, 2022, QI No. jme-20-9736; Manuscript No. jme-20-9736 (R); **Published:** September 22, 2022, DOI: 10.37421/jme.2022.11.15

hardware, optimizing SPION properties and creating forward models to the ill-posed reconstruction problem. Less effort has been dedicated to preprocessing the sensor signals. The high sensitivity of SQUID detection increases the risk of distortion due to far-field, high- and low-frequency corruption. Environmental low-frequency noise is on the same order as NP relaxation and is especially difficult to filter directly.

However, it produces subtle distortions in the signal, which lower the signal-to-noise ratio and limit SQUID sensitivity and SPMR accuracy. We sought to address this problem by capturing far-field magnetic noise with a Magnetometer (MAG) device located within the SQUID apparatus. We developed a filter to parameterize and subtract MAG data from the original signal. Preliminary results indicate that the filter eliminates far-field noise for decreasing NP concentrations. The filter most significantly increases accuracy at very small concentrations of NPs. This is encouraging, as it applies to early stages of disease where cancer-bound particles are limited to small and sparse focal clusters [2].

## Materials and Methods

### Experimental setup

SPMR was conducted using the MagSense™ (Imagion Biosystems, San Diego, CA). It consists of a pair of Helmholtz coils and an array of seven second-order gradiometers. The second-order feature allows a gradiometer to measure change in flux as a function of distance along it, localizing its detection. The electrical current through the gradiometer coil is converted to a voltage by low-temperature SQUID circuitry. The Helmholtz coils apply a uniform magnetic pulse across the sample, causing NPs to align their magnetic domains. Free particles rotate back in Brownian motion immediately, while immobilized (cancer-bound) particles return to zero-configuration by switching their polarity over an order of seconds, by the Néel mechanism. The SQUIDs are turned on after a brief delay and measure the NP field remnant decay for around two seconds.

Thirty pulses were taken for each sample and averaged together. SPION samples were immobilized by drying on cotton swabs and held in plastic cylinders secured with epoxy for durability. Two stage locations were used: center (0 cm, 0 cm, -4 cm) and off-center (0.9 cm, -9 cm, -4 cm). Two environments were tested; no induced noise and wrench-induced low-frequency noise. The wrench was held 30 cm away from the sample stage and oscillated 25 cm in the vertical direction [3].

### Magnetometer

The MAG incorporated in the apparatus consists of a single coil and measures the component of the local magnetic field perpendicular to the coil. Thus, it is sensitive to fields within a wider distance and not robust against environmental interference. This allows the MAG to capture far-field magnetic signals with greater sensitivity and express far-field disturbances at higher amplitude than the gradiometer channels can.

### Preliminary processing (flux jumps, DC offset, 60 Hz)

Preliminary processing addressed flux jumps, the DC bias due to the gradiometric properties of the coil and the 60 Hz electronic frequency and its sinusoidal harmonics. Samples with flux jumps were discarded. Electrical mismatches between signal and SQUID hardware were addressed with a DC offset centered at the mean of the curve. The 60-cycle power line noise and its harmonics were processed using a moving average filter of a window of 0.6 ms [4].

### Processing filter

The filter on each channel consisted of four steps; modelling and subtracting the component of structural relaxation; aligning the MAG curve to the channel curve; setting a subtraction window, subtracting the MAG curve from the channel curve and anchoring the result to the original amplitude; and performing a bi-exponential fit. All processing and analyses were done using MATLAB R2018©.

### Structural relaxation subtraction

Although the decay curve detected by SQUIDs is most influenced by the Néel relaxation of the NPs, it contains both a Brownian factor and a component of decay due to magnetic materials in the environment. This “structural relaxation” is distinct from far-field high/low-frequency noises. In general, NP relaxation is modelled by a multi-term exponential decay model based on the Néel mechanism [5].

$$F = a_0 + a_1 \exp\left(-\frac{t}{a_2}\right) + a_3 \exp\left(-\frac{t}{a_4}\right) + 2 b_i \sin(\varphi_i + \omega_i t)$$

Huang define the terms as follows:  $a_0$  represents the arbitrary DC offset;  $a_1$  represents the remanence field and overall magnetic moment of the sample;  $a_2$  represents the long-decay constant for a SPION;  $a_3$  represents structural relaxation; and  $a_4$  represents the short decay time constant. Structural relaxation was thus modeled as a single-exponential term and subtracted from each curve.

### Parameterizing MAG to channel curves

MAG data were parameterized to the gradiometer curves in order to align the two, such that the MAG signal could be proportionately subtracted. This was organized as a linear transformation where MAG data were scaled to each gradiometer channel's data by a parameter. Parameters were solved through least-squares optimization, minimizing the distance between MAG and gradiometer curves.

### Subtraction window and anchor

A typical sample trace features the initial magnetizing pulse, followed by a rapid decay that is disproportionately affected by the short-term decay constant and 60 Hz power-line noises, despite processing. Because this rapid decay component is time-dependent and mirrored in both MAG and gradiometer channels, we ignored the early time interval by setting a filtering window. Within this window, the aligned MAG curves were each subtracted from corresponding gradiometer curves. To correct the resulting offset, the curve window was anchored to the mean of the last 100 ms of the unfiltered decay curve.

### Bi-exponential fit

To recreate a centered decay curve shape from the corrected data, a final bi- exponential fit was performed, inspired by the Néel model. This aids in image reconstruction.

### HSPMR image reconstruction

The HSPMR image reconstruction method was developed by Huang and uses a multi-start approach to find the best fitting solutions to fit the decay equation. It solves the inverse problem of estimating the location and magnitude (magnetic moment) of a SPION source(s) for a given measurement and magnetic field distribution at the SQUID sensors. We refer further characterization of this method to [6].

## Results

### Far-field magnetic sources dominate MAG detection

MAG decay curves were compared for eight traces at increasing NP concentrations (no induced noise); 0 ug, 5 ug, 10 ug, 20 ug, 50 ug and 100 ug. There was no significant increase (or decrease) in range, mean or median of the data or qualitative change in the curve shape with varying NP concentrations. This confirms that MAG signal is not significantly influenced by the NPs and MAG subtraction will not also eliminate NP signal.

### MAG curve correlates at irregularities with channel curves

Extreme induced low-frequency noise caused visible and isolatable peaks in MAG data. Peaks were defined by neighbouring inflection points, visually confirmed and computationally matched with gradiometer data along the time domain. Overall correlation between MAG and gradiometer data increased significantly for all seven channels. Average cumulative distance between MAG and gradiometer data decreased by over 85% for all channels (Figures 1 and 2) [7].

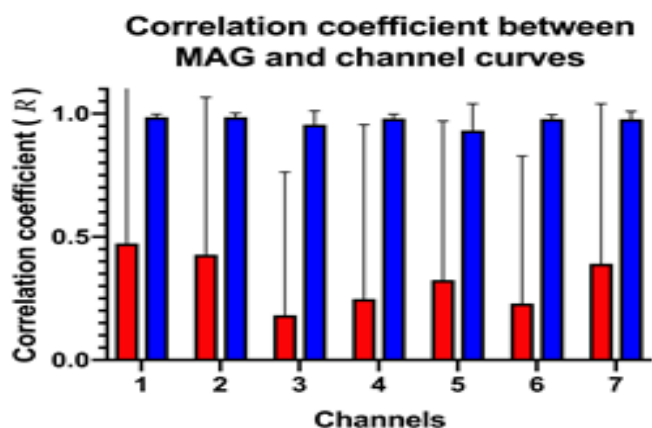


Figure 1. Lot of correlation coefficient between MAG and channel curves before and after parameterization. (Note: ■ MAG: Raw ■ MAG: Corrected pulse-by-pulse).

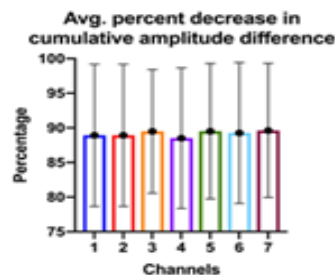


Figure 2. Plot of average percent decrease in the difference in cumulative amplitude between MAG and channel curves, after parameterization.

### MAG alignment and subtraction can be optimized to increase HSPMR reconstruction accuracy

Thirty pulses were taken and averaged, for both center and off-center NP sources. Trials with standard deviation greater than two were discarded. Results were compared with and without filtering. Center; for a 50 ug NP source, the distance off-target decreased by 0.21 cm or 14.93% and magnetic moment decreased by 8.37; for 1 ug, distance off-target decreased by 1.11 cm or 63.76%, though magnetic moment increased by 0.12; for 5 ug, distance off-target increased by 1.97 cm, which was significantly outlying and therefore excluded from analysis. Off-center; for a 50 ug NP source, distance off-target increased by 0.27 cm; for 5ug, distance increased by 0.16 cm; for 1 ug, distance decreased by 1.01 cm (67.68%). Overall, there was a positive correlation between the filter's relative increase in accuracy and decreasing NP concentration (Figures 3-7).

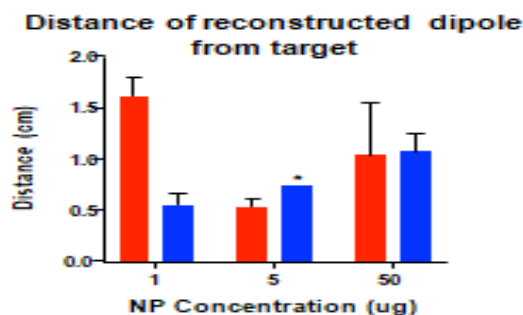


Figure 3. Comparison of the reconstructed dipole distance from the source target for uncorrected and corrected signals across NP concentrations. (Note: ■ Uncorrected ■ Corrected).

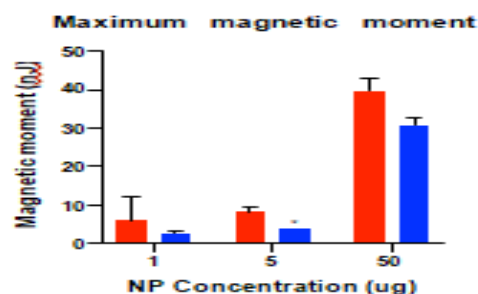
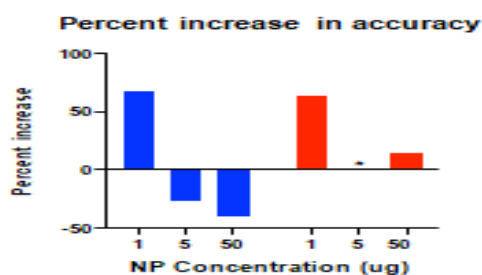
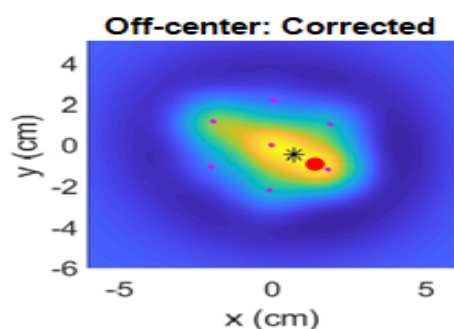


Figure 4. Comparison of maximum detected magnetic moment for uncorrected and corrected signals across NP concentrations. (Note: ■ Uncorrected ■ Corrected).



**Figure 5.** Comparison of percent increase in accuracy (decrease in distance away) after correction, between off-center and center-stage NP sources. (Note: ■ Off-center ■ Center).



**Figure 6.** Field distribution map showing reconstructed location.

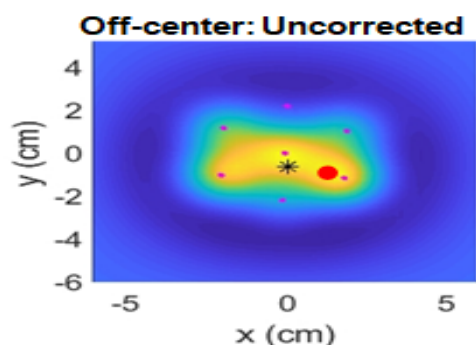


**Figure 7.** Field distribution map showing reconstructed location.

## Discussion

This study addresses the need for a preprocessing filter to improve SPMR sensitivity in the face of subtle but impactful low-frequency artifacts from far-field noise. The filter subtracts far-field noise represented in MAG peaks from corresponding distortions in gradiometer channels. HSPMR reconstruction of decreasing concentrations of NPs located off-center and center-stage shows that the filter works more effectively as NP concentration decreases. Percent decrease in distance off-target was larger at low NP concentrations (~1 ug) for both center and off-center sources. A decrease in magnetic moment confirms the filter increased in relative robustness for lower NP concentrations [8].

For ovarian OVACR3 cells, obtained a concentration of  $2.5 \times 10$  H NPs/cell and obtained a NP dipole density of  $1.5 \times 10$  NP, in preparation. Therefore, the dipole moment per cell is at 0.38 cells.

The weakest phantom with accurate reconstruction used in this experiment featured a magnetic moment of 2131.9 at 4 cm of depth. This would correspond to an SMPR sensitivity of ~ 5610 cells. It is extremely rare for a non-invasive technique to have such a high sensitivity. Our goal is to translate SPMR into the clinic as a method for early tumor detection, diagnosis and staging of disease. Because of its spatial analysis, SPMR has been proposed as a third-line screening method to improve the specificity of other multi-modality procedures used for ovarian cancer detection. SPMR would confirm or reject the presence of a disease too small or sparse to be detected by conventional assays. It would also indicate whether a tumor is small, contained and should be respected or if it is distributed, indicating the need for pervasive or chemotherapeutic treatment. Already more sensitive and specific, if SPMR is continued to be developed, it has the potential to become quicker, easier and more effective than other diagnostic measures in the realm of early tumor detection. Finally, there are critical limitations of this study. Most importantly, it is not comprehensive and uses preliminary data with MAG and SQUID setup. Further testing is necessary in order to validate the conclusions made from the data and to compensate for the unevenness in this study. Similarly, the filter itself is not optimized to its full potential; rather, the data indicate that further optimization of the constrained window as well as the order of filtering steps should be undertaken.

## Conclusion

We present preliminary data on a preprocessing filter aimed at eliminating far-field, low-frequency disturbances to SPMR. This filter incorporates a magnetometer to detect and subtract far-field, low-frequency artifacts from SQUID gradiometer signals. This filter shows promise for significantly increasing SPMR sensitivity at low NP concentrations, which is critical for early stage tumor detection of cancers. Notably, we increased SPMR accuracy at NP concentrations of ~1 ug, which corresponds to a sensitivity of ~ 6000 cells. This is encouraging and indicates the robustness of the filter and the merits of SPMR as an ultra-sensitive, highly specific technology for early tumor detection.

## Acknowledgement

The authors acknowledge the Cancer Prevention Research Institute of Texas (CPRIT)-CURE Summer Program at MD Anderson Cancer Center (MDACC) for funding and supporting Mehdi Baqri. Use of the MagSense™ device and magnetic NPs was part of a collaborative research agreement between Imagination Biosystems Inc. and MDACC. We thank Nick Sowko and Wolfgang Stefan for their scientific advice, support and help.

## References

1. Brown, PO, and Palmer C. The Preclinical Natural History Of Serous Ovarian Cancer: Defining the Target for Early Detection. *PLoS Med* 6 (2009).
2. National Academies of Sciences, Engineering and Medicine. Ovarian Cancers: Evolving Paradigms in Research and Care.
3. Eberbeck, D, Wiekhorst F, Steinhoff U, and Trahms L. Aggregation Behaviour of Magnetic Nanoparticle Suspensions Investigated by Magnetorelaxometry. *J Phys Condens Matter* 18 (2006).

4. Ludwig, F, Heim E, and Schilling M. Magnetorelaxometry of Magnetic Nanoparticles-A New Method for the Quantitative and Specific Analysis of Biomolecules. 2004: 245-248.
5. Flynn, ER, and Bryant HC. A Biomagnetic System for *In Vivo* Cancer Imaging. *Phys Med Biol* 50 (2005): 1273.
6. De, Haro, Leyma P, Todor Karaulanov, and Erika C. Vreel. Magnetic Relaxometry as Applied to Sensitive Cancer Detection and Localization. *Biomed Tech* 5 (2015): 445-455.
7. Huang, Ming-Xiong, Bill anderson, Charles W. Huang, and Gerd J Kunde, et al. Development of Advanced Signal Processing and Source Imaging Methods for Super Paramagnetic Relaxometry. *Phys Med Biol* 3 (2017): 734.
7. Thrower, Sara. A Compressed Sensing Approach to Detect Immobilized Nanoparticles Using Superparamagnetic Relaxometry.(2018).
8. You, Zheng. Space Microsystems and Micro/Nano Satellites.

**How to cite this article:** Baqri Mehdi, Sri Kamal K andala and David Fuentes. "A Preprocessing Filter to Improve Super Paramagnetic Iron Oxide Nanoparticle (SPION)-Based Early Tumor Detection". *J Material Sci Eng* 11 (2022): 15.